COMPOSITE PRESSURE VESSEL DESIGN: INTEGRAL DETERMINATION OF WINDING PATTERNS

Adriaan Beukers, Sotiris Koussios, Otto Bergsma
Design & Production of Composite Structures
Faculty of Aerospace Engineering
Delft University of Technology
Delft, The Netherlands

Keywords: *Filament winding, Patterns, Diophantine equation, Non-Geodesics*

Abstract

The most important issues for the design of composite pressure vessels reflect on the selection of the most suitable rovings (in terms of strength and thickness) and the distribution of the intended number of circuits around the vessel periphery. In this paper we show that dimensioning a pressure vessel and selecting a roving without the simultaneous creation of winding patterns will definitely lead to a less optimal design. The designer should simultaneously ensure tangential pole passage for the rovings, homogenous coverage (by using roving widths according to a predetermined range), and, at the same time, minimise the excess of overwound circuits as compared to the number of rovings dictated by structural analysis. In this paper we provide a methodology for dealing with this contradicting set of demands.

Background

The design procedure for filament wound products can be characterized by a strong interaction between shape determination, structural performance, selection of materials and reinforcement layer architecture [1-3]. Particularly in cases where the intended product is very sensitive to the resulting fibre architecture, the simultaneous determination of appropriate winding patterns and suitable fibre trajectories becomes a necessity. Typical examples of such fibre-architecture-sensitive structures are composite pressure vessels. In this case, a prescribed number of layers or rovings of particular dimensions should not only lead to feasible winding trajectories (occasionally non-geodesics) but also automatically fit into acceptable winding patterns.

Problem identification

In a more concise formulation, the output of the structural design procedure for a composite pressure vessel is usually a minimally required number of particular rovings that should overwrap the mandrel. In [4] the necessity for partially applying non-geodesic winding has been demonstrated. The following step is the determination of a proper winding pattern where the pattern-dictated number of circuits should ideally be the same as the required number of rovings, as dictated by structural analysis [5, 6]. Hence a simultaneous matching is here required.

In regard to structural analysis [5-7], pattern creation [8, 9] and fibre path determination [10-12], an extensive collection of references can be found. Here, we have just mentioned a few. However, little attention has been paid to the interaction between these design tasks. In [13, 14] some examples can be found. Particularly in the case where partial non-geodesic winding is applied, automatic matching of patterns to the structural layout becomes increasingly complicated. A pattern must be achieved for which the underlying number of windings is not unacceptably bigger than the required number of rovings, the winding angle at the polar areas should be equal to 90° [15], the utilized friction must not exceed the available one, and the width of the applied rovings must be realistic, preferably within a prescribed range. The solution to this problem requires an integral approach. The perfect match has to be obtained in the form of the appropriate {friction, roving width} combinations.

Proposed solution

In this paper we provide a methodology for automatically creating suitable winding patterns for pressure vessels, regardless the presence of non-geodesic fibre trajectories.

The first issue that should be tackled is the degree of reinforcement. This definition reflects on the strength per unit of width of a roving that is made out of a particular material, with a particular thickness. We have chosen for this definition, because at the end, the roving width itself is not a decisive parameter for the structural performance; one can e.g. apply 200 rovings with a width of 1 [mm] or 20 rovings with a width of 10 [mm]. The most important item is that the strength / roving thickness combination must ensure an integer number of overwound layers. Amazingly, this constraint has never been analyzed in a systematic way. Most pressure vessel designs do not comply with this rule.

Next, with the proper roving data, we must identify which parameters influence the so-called turnaround angle of a winding. This quantity is the angular propagation between two neighbouring circuits. Depending on the range and the magnitude of the involved friction (for the creation of the non-geodesic parts of the roving trajectory), the turnaround angle will obtain distinctive values. On the other hand, the creation of either a perfect leading or lagging pattern requires prefixed values for the turnaround angles. These values are based on the selected roving properties (strength & thickness) and the range for the roving width itself (this does only affect the pattern, not the structural performance). The pattern-dictated angular propagations should match the turnaround angles as created by the fibre paths. However, in the general case, it is not unlikely that a match can not be obtained. For example, if the range of the fibre-path-generated turnaround angles lays outside the range of the pattern dictated ones, some additional turning around of the roving at the polar areas might be inevitable. Hence, the methodology is split into two parts; firstly, a proper investigation is carried out to identify possible matching and secondly a fine-tuning is performed to create perfect matching by means of additional turnaround. Alternatively, a refined search can be performed for exactly pin-pointing the best roving width or amount of friction that will lead to the automatic coincidence of the pattern dictated and roving dictated turnaround angles.

Outline

The link between favourable structural performance (sufficient number of rovings) and economic production (least excess of wound circuits) is established by a comparison of the amount of reinforcement and the number of overwound circuits. In section 2 we provide a short overview regarding the determination of the minimally required number of rovings.

Next, in section 3 we emphasize the importance of proper winding patterns and accordingly we define the main parameters that lead to such patterns.

In section 4, an outline is given regarding the calculation of the turnaround angles and the determination of the required number of windings, specifically adjusted to a particular number of overwound layers. The latter requires dedicated selection of appropriate material / roving thickness combinations.

With the entire set of pattern related parameters, the coupling to the structural performance requirements is explained in section 5. In addition, we outline the methodology for finally obtaining the best patterns possible. The most appropriate patterns are obtained after a fine-tuning procedure, based on either additional turning around at the poles or a refined search in the {friction, roving width} space.

The paper ends with a short presentation of the conclusions in section 6, where we additionally provide some recommendations.

2 Required number of rovings

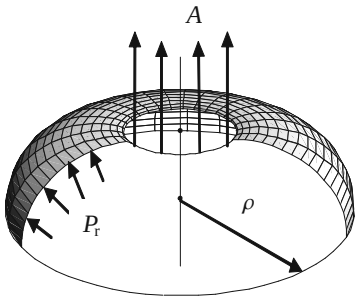

Fig. 1. Loads on, and geometry of a pressure vessel

Since the determination of feasible winding patterns does strongly rely on the number and dimensions of the applied rovings, it is convenient to shortly outline how these parameters affect the strength of a particular pressure vessel design, which is schematically given in figures 1 and 2.

2.1 Axial equilibrium

In figure 1, a rotationally symmetric shell is given that is loaded by a uniform axial force distribution A and internal pressure P_r. The axial equilibrium of forces, at a datum ρ is given by [4, 5]:

$$FN_f \cos\alpha \cos\beta = P_r \pi \rho^2 + A \qquad (1)$$

where the total number N_f of rovings crossing the periphery are loaded by a force F. The angles α (winding angle) and β (related to the meridian slope) are given in figure 2.

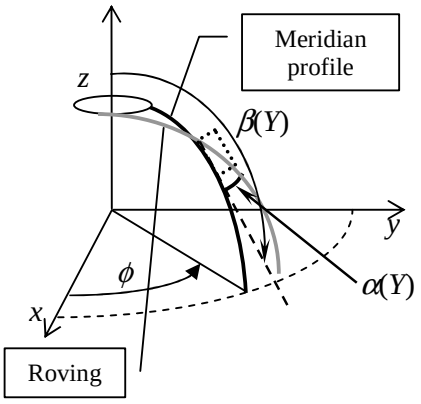

Fig. 2. Geometric parameters of a shell meridian

The radius ρ belongs to the range $[\rho_0, \rho_{eq}]$. A more elegant way for writing equation (1) is:

$$a \cos\alpha \cos\beta = k_a + Y^2 \qquad (2)$$

where:

$$Y = \frac{\rho}{\rho_0}, \qquad a = \frac{FN_f}{\pi P_r \rho_0^2}, \qquad k_a = \frac{A}{\pi P_r \rho_0^2} \qquad (3)$$

In addition, we introduce:

$$Z = \frac{z}{\rho_0} \qquad (4)$$

The most convenient type of fibre placement for pressure vessels reflects on geodesic winding, governed by the Clairaut equation:

$$\sin\alpha = \frac{\rho_0}{\rho} = \frac{1}{Y} \qquad (5)$$

The second angle in equation (2), β, is given by:

$$\cos\beta = \frac{z'(\rho)}{\sqrt{1+z'^2(\rho)}} = \frac{Z'(Y)}{\sqrt{1+Z'^2(Y)}} \qquad (6)$$

With the dimensionless coordinates $\{Z, Y\}$ and equations (1), (5) and (6), the differential equation for the optimal meridian profile can be formulated as [4, 5]:

$$Z'(Y) = \pm \frac{k_a Y + Y^3}{\sqrt{a^2(Y^2-1) - (k_a Y + Y^3)^2}} \qquad (7)$$

At the equator, the meridian profile will have a vertical slope, hence $\cos\beta = 1$ and $Z'(Y)$ = infinity. From equation (2) or alternatively, by setting the denominator of (7) equal to zero, we obtain:

$$a = Y_{eq}\left(\frac{k_a + Y_{eq}^2}{\sqrt{Y_{eq}^2 - 1}}\right) = \frac{k_a + Y_{eq}^2}{\cos a_{eq}} \qquad (8)$$

Combination of equations (2) and (3b) leads to:

$$FN_f = \frac{Y_{eq}}{\sqrt{Y_{eq}^2 - 1}}\left(A + \pi P_r \rho_0^2 Y_{eq}^2\right) \qquad (9)$$

From this expression, one can determine the required number of rovings / bundles / tows N_f where each of them has a strength F. The input parameters for this derivation are just two in number: the radial aspect ratio (Y_{eq}) and the axial load A.

2.2 {*q*, *r*} parameterisation

As outlined in the previous subsection, the meridian profile depends on a geometric parameter (radial ratio) and the axial force. As described by equation (9), the axial load *A* can directly be compared to the total axial load induced by internal pressure, on the projected surface at the vessel equator:

$$r = \frac{A}{\pi P_r \rho_0^2 Y_{eq}^2} = \frac{k_a}{Y_{eq}^2} \tag{10}$$

The geometric parameter (Y_{eq}) can also be expressed in a more convenient way. To enhance this, we should first look at the denominator of equation (7). One value where it nullifies is $Y = Y_{eq}$. The second real value providing zero is generally slightly bigger than 1 [4, 5, 15]. We will call this Y_{min}. The ratio of the minimum and maximum radius is expressed by:

$$q = \left(\frac{Y_{eq}}{Y_{\min}} \right)^2 \tag{11}$$

Plugging expressions (10) and (11) into (8) leads to:

$$a = \frac{q^{3/2}(1+r)Y_{\min}^3}{\sqrt{qY_{\min}^2 - 1}} \tag{12}$$

Substitution of this result into the denominator of (7) and solving for zero leads to:

$$Y_{\min} = \frac{1}{\sqrt{q}} \sqrt{\frac{1+q+2qr+q^2(1+r)^2}{1+q+2qr}} = \frac{Y_{eq}(q,r)}{\sqrt{q}} \tag{13}$$

Now we can substitute this expression into (12) to obtain a {*q*, *r*}-based expression for the axial load [15]:

$$a = \frac{[1+q+2qr+q^2(1+r)^2]^{3/2}}{q(1+q+2qr)} \tag{14}$$

With the original definition for *a* (equation (3b)), one can finally obtain:

$$FN_f = \pi \left(\frac{[1+q+2qr+q^2(1+r)^2]^{3/2}}{q(1+q+2qr)} \right) P_r \rho_0^2 \tag{15}$$

From this equation it becomes clear that the degree of reinforcement is linear to the internal pressure while increasing in a quadratic fashion with the reference opening radius. With this derivation, the expression for the first pattern related parameter, the number of rovings, is established.

3. Winding patterns

3.1 Why a pattern?

The axial equilibrium of forces is able to provide the required number of fibre bundles, according to their strength. An important assumption here is that the created laminate is homogeneous in terms of equatorial thickness distribution. This implies that the rovings must be equally distributed, without leaving any gaps or creating excessive overlaps.

The creation of winding patterns makes obviously only sense when the same roving placement procedure is repeated. Therefore, it only applies on rotationally symmetric objects, at least, as formulated in this paper. An example of a few windings on a typical pressure vessel is given in figure 3:

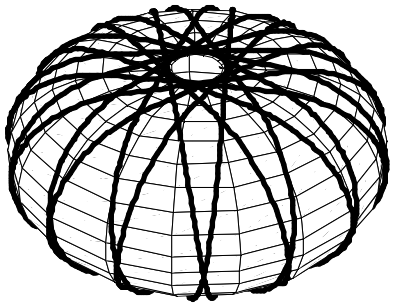

Fig. 3. Pattern on a pressure vessel (one round of circuits completed)

One can observe that the vessel periphery is divided into a certain number of partitions (*p*). After completing this round, the next wound circuit should lay exactly next to very first one; this placement will

initiate the second round of windings. After (k) rounds the entire periphery should be covered. It is previously mentioned that, after completing the first round, the subsequent circuit lays adjacently to the very first wound circuit: this holds true in the case where the manufacturer intents to create a single layer of rovings. In the case of multiple layers (d >1) the overlap should preferably be (1/d). For example, if two layers are desired, the overlap after the first completed round must 50%; in the case of 3 layers this should 33.3% and so on.

3.2 Pattern conditions

In figure 4 we provide a schematic representation of how a pattern works. The figure can be regarded as the top view of a rotationally symmetric mandrel, covered with a particular number of circuits.

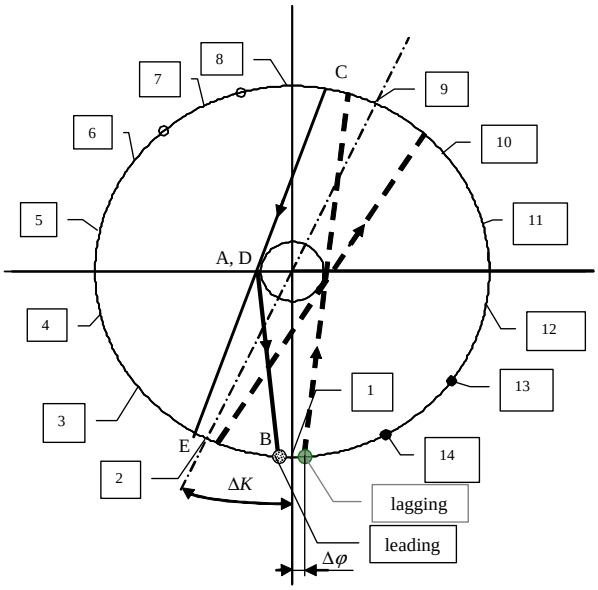

Fig. 4. Schematic representation of a winding pattern

Let us assume that the winding procedure begins on the upper half of the mandrel. When passing the equator in a downward direction, we indicate the circuit by a black dot. The white dots reflect on the upward passage of the equatorial periphery. The visible roving trajectories are represented by the continuous black lines; the rovings, placed on the lower hemisphere are given by doted lines.

Starting at point A, the roving crosses for the first time the equator (B) and proceeds to the lower (non visible) part. The second crossing with the equator takes place in an upward direction (C). After this, the roving passes the polar opening (D). At this point, the second circuit (winding) is started, which proceeds towards point (E). The angular difference between points E and B (ΔK) is the first major parameter that determines the winding pattern. The second one is the width of the roving itself. Since the roving does not cross the equator in an exactly perpendicular fashion but with a winding angle α_{eq}, (see also figure 3) the roving width must be corrected according to:

$$b_{pr} = \frac{b_{roving}}{\cos\alpha_{eq}} \tag{16}$$

where α_{eq} is given by equation (5) for $Y = Y_{eq}$. The arc covered by the roving width is $\Delta\varphi$.

Suppose now that we aim to create a single wound layer. In this case, circuit #15 must be placed exactly before or after the first circuit (the terms before or after are defined according to the direction in which the circuits propagate). The first way of placement is referred to as lagging, and the second as leading. If e.g. a number of two fully closed layers is required, the overlap should be 50% and so on.

Let the angular difference between two adjacent circuits be ΔK. This angular value fits p times in the equatorial periphery. In every partition ΔK, a number k of roving arcs $\Delta\varphi$ will fit. For a lagging pattern, the p-th circuit should be placed just before winding #1, and for a leading pattern the roving #p+1 should be placed just after #1. Depending on the desired number of layers, a certain overlap is required. Hence [13]:

$$\begin{aligned} (p+1)k - n &= \frac{1}{d} \qquad leading \quad pattern \\ pk - n &= -\frac{1}{d} \qquad lagging \quad pattern \end{aligned} \tag{17}$$

Although intuitively correct, we should keep in mind that the participating parameters are all integers. Therefore, an integer solution for equation (17) is impossible. The correct way for providing the winding equations is [8]:

$$\begin{aligned} (p+1)kd - nd &= 1 \\ pkd - nd &= -1 \end{aligned} \tag{18}$$

where *nd* is treated as a single integer parameter here. These equations have only an integer solution when the involved parameters do not have a common divisor.

3.3 Pattern parameters

As previously indicated, there is an angular difference ΔK (ϕ-difference, figure 2) between two adjacent windings. For convenience this difference must be limited into the 2π interval [4, 8, 13]:

$$\Delta K = \min[|\mathrm{mod}(\Phi, 2\pi)|, |\mathrm{mod}(\Phi, -2\pi)|] \quad (19)$$

where Φ stands for the angular propagation between two adjacent circuits, as provided by the roving path calculation (for details see [15] and section 3.4 in this paper). The second important parameter is the arc length, occupied by a single roving:

$$\Delta\varphi = \frac{b_{roving}}{\rho_0 Y_{eq} \cos\alpha_{eq}} = \frac{b_{roving}}{\rho_0} \frac{1}{\sqrt{Y_{eq}^2 - 1}} \quad (20)$$

Now we are able to determine the pattern parameters:

$$\begin{aligned} p &= IP\left(\frac{2\pi}{\Delta K}\right) \\ k &= C\left(\frac{\Delta K}{\Delta\varphi}\right) \\ nd &= C\left(d\frac{2\pi}{\Delta\varphi}\right) \end{aligned} \quad (21)$$

Where *IP* stands for "integerpart"; the biggest integer contained in the argument, and *C* for "ceiling" the smallest integer containing the argument. We do not use here the exact definitions that also deal with negative arguments since the entire set of them is here positive. The reason for choosing the *C* function for *k* and *nd* is to ensure a small overlap of the rovings at the equatorial periphery (which provides the largest space to be covered). In the unlikely event where Φ and the roving width do already provide integer values for *p*, *k* and *nd*, the overlap within one layer becomes equal to zero.

4 Structural design & pattern creation

4.1 Angular ϕ-propagation

In [15] we have shown that the production of composite pressure vessels exclusively relying on geodesic trajectories is not possible, in particular for small *q*-values. To cope with this, we have proposed the application of friction for the generation of partially non-geodesic winding trajectories. The main goal of this application is the creation of a winding angle equal to 90° when passing the polar periphery; this enhances continuation to the next wound circuit. The friction has been introduced in the form of a step function, where, depending on the step length (non-geodetically placed roving length) and height (amount of friction), the winding angle could possibly become less than 90° or exceed this value. In the first case, continuously winding of the object is not possible, in the second case the path will "stick" on a singularity; it will follow the periphery of the mandrel at some altitude. Non-geodesic winding takes usually place near the poles (end domes) of the vessel since the structural performance reduction over there can be alleviated by the (usually applied) flanges. The adapted step function for the friction is [15]:

$$\begin{aligned} &\mu(\gamma, m, \theta) = 0 \qquad 0 \le \theta \le \gamma \\ &\mu(\gamma, m, \theta) = m \qquad \gamma \le \theta \le \frac{\pi}{2} \end{aligned} \quad (22)$$

where θ is an elliptic coordinate, defined as [4, 5]:

$$\begin{aligned} &Y^2(\theta) = Y_{eq}^2 \cos^2\theta + Y_{\min}^2 \sin^2\theta \\ &where \qquad -\frac{\pi}{2} \le \theta \le \frac{\pi}{2} \end{aligned} \quad (23)$$

In equation (22), the parameter *m* is the step height and γ the θ-range over which the friction is applied. The resulting non-geodesic winding angle distribution is denoted as [15]:

$$\alpha_{ng}(q, r, \gamma, m, \theta), \qquad 0 \le \theta \le \frac{\pi}{2} \quad (24)$$

Based on this expression, the associated ϕ-propagation is then given by [4, 15]:

$$\phi(q,r,\gamma,m,\theta) = \\ = \int_{s=0}^{s=\theta} \sqrt{\frac{G(q,r,\theta)}{E(q,r,\theta)}} \tan[\alpha_{ng}(q,r,\gamma,m,\theta)] \quad (25)$$

where G ($=Y'^2+Z'^2$) and E ($=Y^2$) are coefficients of the first fundamental form (for the derivation of $Z(q, r, \theta)$ we refer here to [15]).

The $[\gamma, m]$ combinations providing $\alpha_{ng}(q, r, \gamma, m, \pi/2) = \pi/2$ (tangential roving placement at the pole) are given by a function $m(\gamma)$. In figure 5, we provide an example of such a graph for [q = 3, r = 0].

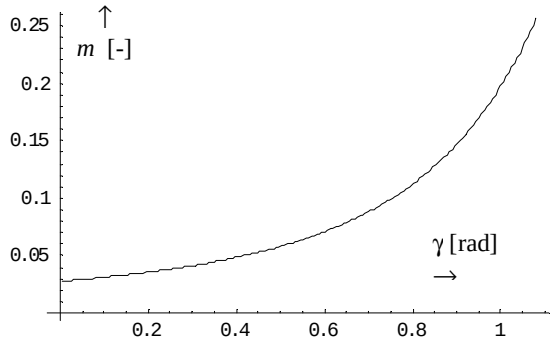

Fig. 5. Friction coefficient m for tangential fibre placement at the pole as a function of the step interval γ

As a complete wound circuit passes four times the vessel meridian, the total turning around Φ is given by:

$$\Phi(q,r,\gamma) = 4\phi[q,r,\gamma,m(\gamma),\pi/2] = \\ = 4\phi[q,r,\gamma,\pi/2] \quad (26)$$

Since q and r are fixed (shape and load parameters), the only way to vary Φ is to choose for another γ-value.

4.2 Total number of circuits

The second pattern parameter combination, the roving dimensions and implicitly the minimum number of rovings (for structural integrity) have to be related to the pattern parameters. With a given roving strength F, the required number N_f of rovings that cross the equator is given by equation (15). As depicted in figures 3 and 4, a wound circuit will cross the equator twice, therefore we can write:

$$N_f = 2nd \quad (27)$$

At the same time, the roving strength is given by:

$$F = \sigma bt \quad (28)$$

where b is the roving width, t the thickness and σ the allowable stress. Combination of (15), (27) and (28) leads to:

$$nd = \frac{1}{2}\left(\frac{[1+q+2qr+q^2(1+r)^2]^{3/2}}{q(1+q+2qr)}\right)\left(\frac{P_r}{\sigma}\right)\left(\frac{\pi\rho_0^2}{bt}\right) \quad (29)$$

This equation does in essence summarise the pressure vessel design procedure. Namely, the total number of windings (that refer to possible patterns) is the result of the shape and axial load parameters [q, r], the relative fibre strength (as compared to the internal pressure) and the relative roving cross section (as compared to the surface of the polar opening).

4.3 Number of layers

Since the number of overwound layers must be an integer number, we will prove here that the strongest fibre does not automatically imply the achievement of the optimal pressure vessel. Substitution of equation (13) into (20) leads to a [q, r]-defined expression for n. For simplicity, we have used here (21c) without the ceiling function since the aim is to derive an integer d. To achieve this, we substitute the obtained expression into equation (29) and solve for d. The result is:

$$d = \left(\frac{\rho_0}{t}\right)\left(\frac{P_r}{\sigma}\right)\left(\frac{[1+q+2qr+q^2(1+r)^2]^{3/2}}{4q^2(1+r)\sqrt{1+q+2qr}}\right) \quad (30)$$

Note that the result is independent of the roving width. Obviously, the vessel strength is determined by the strength and thickness of the created laminate and not by the width of the individual rovings; a large number of narrow rovings provides the same result as a small number of broad rovings.

Let us assume now that P_r and ρ_0 are given. The challenge now is to locate proper σt products

that are able to provide integer *d*-values. Rewriting of equation (30) leads to:

$$\sigma t(q,r,d) = \frac{P_r \rho_0}{4d}\left(\frac{[1+q+2qr+q^2(1+r)^2]^{3/2}}{4q^2(1+r)\sqrt{1+q+2qr}}\right) \tag{31}$$

This means that for a particular vessel shape (defined by [*q*, *r*]), size (defined by ρ_0) and pressure (P_r), one should choose a roving of particular strength and thickness to achieve an integer number of layers. Note that the result of equation (31) is actually the roving strength per unit width.

5 Matching procedure

5.1 Angular propagation criterion

During winding (according to some friction distribution), the angular difference between two circuits is given by equation (19). This value should match the angular propagation, as required by the winding pattern (equation (32)). To determine this, we recall equations (21) where we assume now that the integer quantities are given. Hence, the round-off to integers is here not necessary. Plugging these expressions into respectively equations (18a) and (18b) leads to:

$$\begin{aligned} \Delta K^{leading}_{required} &= \frac{2\pi}{p+1}\left(1+\frac{1}{nd}\right) \\ \Delta K^{lagging}_{required} &= \frac{2\pi}{p}\left(1-\frac{1}{nd}\right) \end{aligned} \tag{32}$$

5.2 Polar passage

As outlined in subsection 4.1, the main parameter for determining Φ (which in its turn determines Δ*K* as provided by the roving path, equation (19)) is γ (equation (22)). For every γ there is a friction value *m* such that the winding angle during pole passage is exactly equal to 90°. Hence, the friction should belong to the corresponding curve, as depicted in figure 5. For convenience, the graph can be used in a discretised form during the pattern determination procedure (due to the discrete solution procedure for determining this curve, see [15]).

5.3 Pattern selection

Next to the γ-vector, the designer must select a range for the applicable roving width (e.g. 2 [mm] ≤ *b* ≤ 10 [mm]). The *b*-interval is then divided according to a particular increment (e.g. 0.1 [mm]). For every {*b*, γ} combination, the corresponding $\Delta\varphi$ (equation (20)) and thereof the *nd* (equation (21c)) can now be determined. Combination of equations (26), (19) and (21a, 21b) leads to the quantification of *p* and *k* respectively. The obtained integer-combinations are then plugged into equation (18) to check which ones do lead to a pattern (the result should respectively be +1 or -1). The selected integer combinations are then substituted into equation (32) to determine which angular propagation can generate the found pattern in a perfect way (no round-off). Every "successful" combination is identified by its {*b*, γ} vector. For a "successful" {*b*, γ}, the path-generated Δ*K* can be calculated with the aid of equation (19). The result is then compared to the angular propagation, as provided by (32).

5.4 Refinement

In general, the results of (32) and (19) are not exactly identical. At the *b*-value where this difference is the smallest, the exact angular propagation (as dictated by (32)) can be obtained by tow different ways:

1. Additional turning around at the polar areas (usually in the order 0.1°). The designer should be aware that the correction should be positive; hence it should tend to enlarge the Φ-quantity.
2. In the vicinity of the pattern-generating {*b*, γ} vector, search for a γ or *b*-value that is able to provide an exact Δ*K* match. Condition: the results of equation (19) and (32) should be identical. The proper γ or *b*-value can be found by standard root searching procedures.

6 Conclusions

In this paper we have presented a methodology for the integral determination of winding patterns, as part of the design procedure for composite pressure vessels. The main issues tackled here are the appropriate selection for the roving materials and dimensions in such a way that the required number

of overwound layers is an integer number, and the definition of winding patterns that enable the realisation of the minimum number of circuits while still complying with structural integrity demands.

After a short outline regarding the roving-loads equilibrium for filamentary pressure vessels, the minimally required number of (particular) rovings has been determined. Next, the theory for the construction of winding patterns has been explained, followed by the identification of the associated deterministic parameters. As the main parameters reflect to the roving width and the turnaround angle, a procedure is outlined where the pattern related turnaround values are matched to the path–generated angular propagations. An important constraint here is the a-priori selection of suitable rovings in terms of mechanical properties and dimensions for obtaining an integer number of overwound layers.

For the derivation of the roving path geometry, we assumed here partially non-geodesic winding where the friction distribution is given in the form of step function. Due to this generic approach, the complete range from entirely geodesic to 100% non-geodesic fibre placement can be covered. At the same time, the provided friction distributions ensure perfectly tangential polar passage for winding continuation (see also [15]).

Perhaps the most important contribution of this paper is the derivation of an equation for the a-priori selection of the perfect strength / thickness combinations for the utilised rovings; these should lead to an integer number of layers while exactly matching the strength requirements. In addition, it is proven here that selecting the strongest roving does not always lead to the lightest solution.

With the given friction distribution and roving characteristics, the automated pattern search and refinement procedure shows favourable properties; it is fast, straight forward, reliable and provides the entire data range for allowing the designer to decide which patterns will fit the manufacturing demands in the best way possible. The provided results collection consists of the best roving (in terms of material and thickness), number of required windings, roving width (belonging to a predetermined range), and amount of friction. In addition, depending on the parameter selection for achieving the winding pattern (fine-tuning), one can choose between additional turnaround, slightly modified roving width (which in practice makes no difference) or slightly modified friction values (that still belong to the curve providing perfect passage towards following wound circuits). In particular, consideration of equations (31) and (32) provides a usable tool for better pressure vessel designs.

As a part of future research, the constructed algorithms have to be generalised in such a way that they will become parameterisation-independent. For this approach one can utilise the coefficients of the first fundamental form, as provided by the differential geometry branch.

References

[1] Beukers A, Hinte E van. *Lightness: The inevitable renaissance of minimum energy structures.* Rotterdam: 010 Publishers, 1998.

[2] Peters ST, Humphrey WD, Foral RF. *Filament Winding Composite Structure Fabrication.* Covina CA: SAMPE International Business Office, 1999.

[3] Rosato DV, Grove CS. *Filament winding: its development, manufacture, applications, and design.* Polymer engineering and technology. New York: Interscience, 1964.

[4] Koussios S. *Filament Winding: a Unified Approach.* PhD Thesis Report. Desing & Production of Composite Structures, Faculty of Aerospace Engineering, Delft University of Technology. Delft University Press, 2004.

[5] Jong de Th. *A theory of filament wound pressure vessels.* Report LR-379. Structures and materials laboratory, Faculty of Aerospace Engineering, Delft University of Technology. Delft, April, 1983.

[6] Vasiliev VV, Krikanov AA. New generation of filament-wound composite pressure vessels for commercial applications. *Composite Structures* 2003: 62: 449-459.

[7] Koussios S, Bergsma OK. Analysis of Filament Wound Pressure Vessels Considering the Laminate Thickness Variation through the Meridional Direction. In: *Proceedings of the 14th International Conference on Composite Materials.* San Diego, CA, July 2002.

[8] Johansen BS, Lystrup A. CADPATH: a complete program for the CAD-, CAE- and CAM-winding of advanced fibre composites. *Journal of Materials Processing Technology* 1998: 77: 194-200.

[9] Liang YD. A simple filament winding pattern generation algorithm. In: *Proceedings of the 28th International SAMPE technical conference,* 1996: 1027-1039.

[10] Hongtao Su. Modelling stable filament winding on general curved surface. In: *Proceedings of the 31st SAMPE technical conference,* October, 1999.

[11] Liang YD, Zou ZQ, Zhang ZF. Quasi-geodesics- a new class of simple and non-slip trajectories on revolutional surfaces. In: *Proceedings of the 28th International SAMPE technical conference,* 1996: 1071-1079.

[12] Marchetti M, Cutolo D, Di Vita G. Filament winding of composite structures: validation of the manufacturing process. In: *Proceedings of the 7th International Conference on Composite Materials*, 1989; 7: 135-140.

[13] Koussios S, Bergsma OK. Winding Pattern Determination for Pressure Vessels Comprising Fibre Bundles of Finite Dimensions. In: *Proceedings of the 14th International Conference on Composite Materials.* San Diego, CA, July 2002.

[14] Koussios S, Bergsma OK. Automatic Optimal Pattern Generation for Filament Winding Applications. In: *Proceedings of the 18th Annual Conference of the American Society for Composites.* Gainesville, FL, October, 2003.

[15] Koussios S, Beukers A, Stathis PT. Manufacturability of Composite Pressure Vessels: Application of Non-Geodesic Winding. In: *Proceedings of the 16th International Conference on Composite Materials.* Kyoto, Japan, July 2007.